CHAPTER 3

GPR DATA PROCESSING

Unprocessed GPR data often yield fairly good quality subsurface images, however the data may be difficult to interpret. Enhanced processing can improve image clarity as well as spatial and temporal resolution. GPR data in general can be stored in the seismic standard SEG-Y format and processed using seismic reflection software commonly used in the oil and gas exploration industry (Udphuay et al., 2010).

This chapter presents the data processing and its results of the GPR data sets from Wat Pan Sao and Wiang Kum Kam. The GPR data from both areas were processed using VISTA® 2D/3D Seismic Processing Software version 7.0. The GPR processing steps and descriptions are displayed in a flowchart in Figure 3.1.

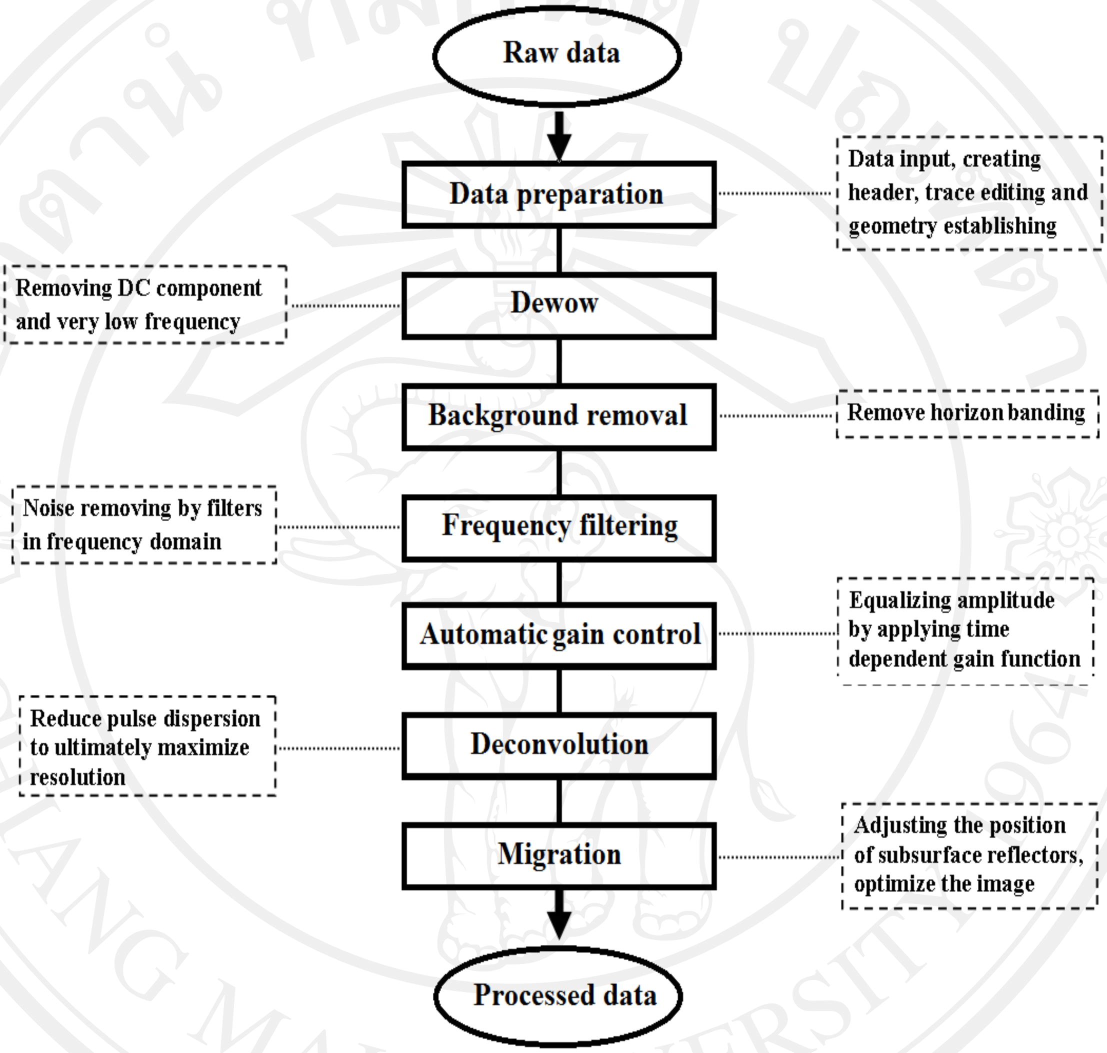

Figure 3.1. The GPR data processing steps and descriptions.

3.1 Data Preparation

Format of input GPR data must be appropriate to the requirement of the processing software and then processing can be applied to the GPR data. This work, SEG-Y format GPR data are required for VISTA® 2D/3D Seismic Processing Software. Header was created for input data to describe characteristic of that data (i.e. trace's name, sample rate, number of samples) and conveniently used in processing. Trace editing was performed to adjust number of traces per one unit distance to the same number for all GPR survey lines. Geometry of GPR data is an importance, must be established to obtain accurate position of each GPR data trace. Accurate positions of data traces yield correct images of subsurface structure after finishing the processing stages.

Thermal drift, electronic instability, cable length differences and variations in antenna air gap can cause jumps in the first arrival time which is usually referred to as the time-zero point (Olhoeft, 2000; Nobes, 1999; Young et al., 1995). This affects the position of the ground interface in GPR section. The time sequence of later events was shifted away from the time zero (Figure 3.2). Then, recorded traces require adjusting to a common time-zero position before applying other processing methods. Time zero correction can be achieved by shifting traces or section to the zero time. The first of the signal would be considered as zero time (i.e. the air wave first break point or first negative peak of the trace).

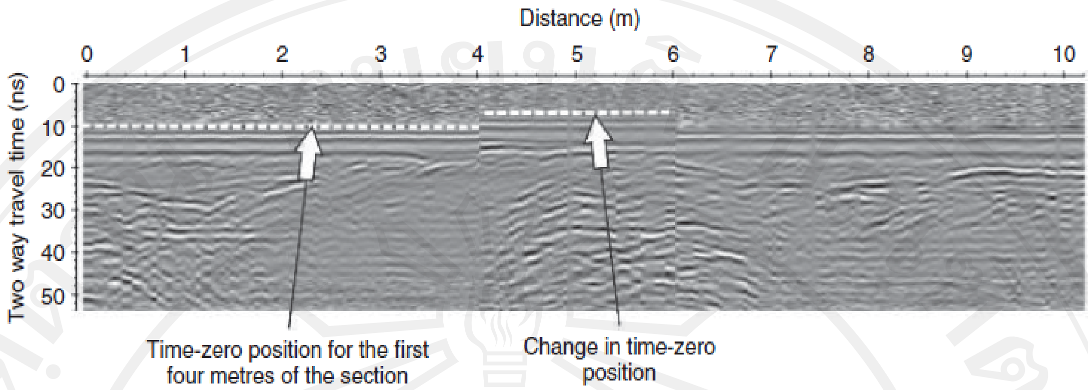

Figure 3.2. Example zero time variation. (From Harry, 2009).

3.2 Dewow

Dewow filter is used to remove the DC component (wow component) or low frequency trend from the GPR data (Dougherty et al., 1994). Wow is caused by DC component or a low frequency trend adds to the recorded signal by early arrivals and/or inductive coupling effects. Dewowing can be performed by reducing the data to a mean zero level and allows positive–negative amplitude to be used in the recorded traces (Figure 3.3). If dewow is applied incorrectly, the data will contain a decaying, low-frequency component which distorts the whole trace. Fortunately, most modern GPR systems now apply dewow to each trace automatically with the filter parameters set to the optimal conditions. If a manual dewow correction is required, it is good to perform DC subtraction first and then use a median filter with a short filter window (typically the same length as the GPR pulse wavelet) and/or a low-cut filter with a cutoff frequency that is below the bandwidth of the recorded data (Gerlitz et al., 1993, Harry, 2009).

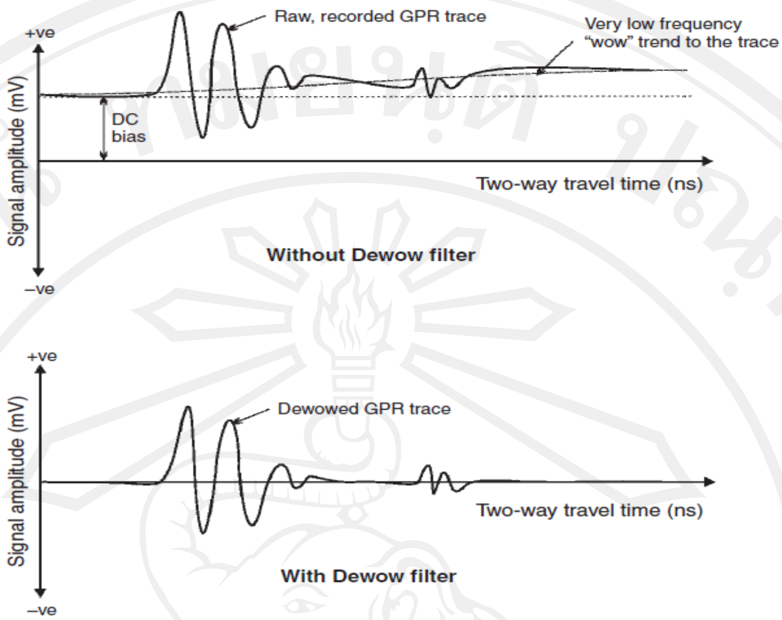

Figure 3.3. GPR signal before applying dewow filter (top) and after applying a dewow filter (below). (From Harry, 2009).

3.3 Background Removal

Background in this study is referred to as continuous flat reflections caused by breakthrough between the shielded antennas and by multiple reflections between the antennas and the ground surface (Daniels, 2004). Background removal process can be achieved by calculating the average amplitude for each GPR profile, and then subtract that average amplitude from data traces in that profile. The average amplitude at the time or sample which background occurs would present high amplitude while another time or sample present very low amplitude. Subsequently, subtracting can remove background effectively.

3.4 Frequency Filtering

EM wave originated from the environment and from devices such as cell phone, radio and transmitter can be recorded together with the GPR data (Add reference here). The waves from these devices characteristic high frequency noise in the GPR profile. These unwanted EM wave signal need to be removed from the data by using various filters.

Low-, high-, and band-pass filters (frequency domain filters)

Low-pass filter allows low frequency components pass and removes high frequencies (good for noise). High-pass filter performs opposite way from the low-pass filter (good for removing signal drift and low frequencies). Band-pass is a combination of both high- and low-pass filters and lets through a specific range of frequency components that are defined by a 'pass region' (Harry, 2009). Band-pass filters are very common and there are a range of types, each with different shaped filter operators that define the shape and form of the pass region (Figure 3.4).

Wave-number domain filter (FK filter)

Wave-number domain filter or FK filter is equivalent to their temporal counterparts in that they convert the data from the distance domain to the wave-number domain. In essence, the wave number represents the spatial size, in meters, of the features in the data. High wave-numbers relate to small, spatially restricted responses (clutter, diffractions, etc.) whilst low wave-numbers are associated with large continuous, spatially coherent responses such as flat-lying reflectors (Harry, 2009).

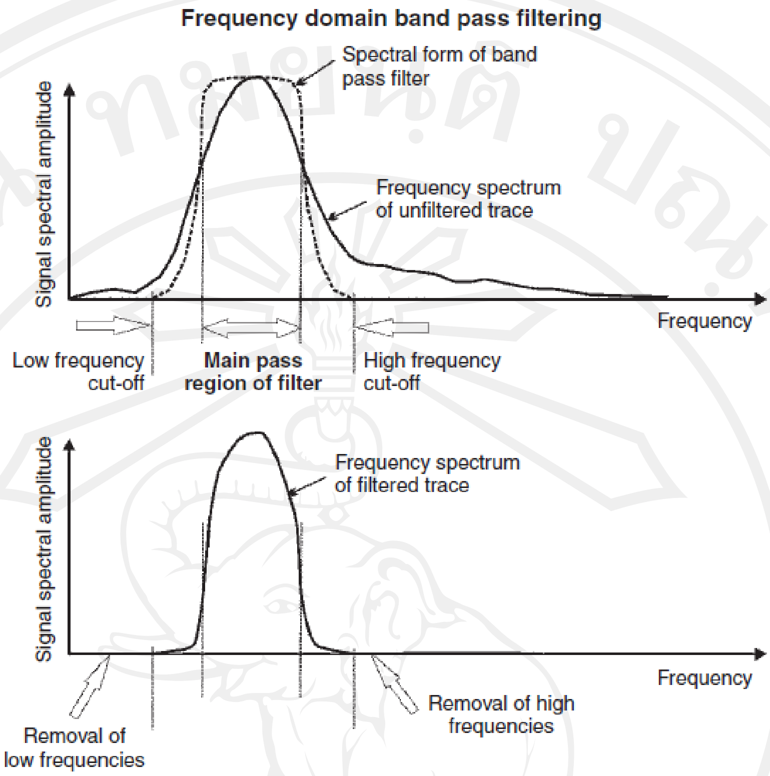

Figure 3.4. Simple band-pass filters in the frequency domain. (From Harry, 2009).

3.5 Automatic Gain Control

Recorded GPR data present high amplitude only at shallow part section and it requires conditioning before visual display. Equalizing amplitudes can be achieved by applying a time dependent gain function compensates for the rapid fall off in GPR data from deeper depths (Figure 3.5). Automatic gain control (AGC) is referred to as a method time-variant equalization (Harry, 2009). Scale factor for a given window is calculated and applied to the sample at the center of window. Then the window slide down one sample and the process is repeated. Hence, each sample has a slightly different scale factor.

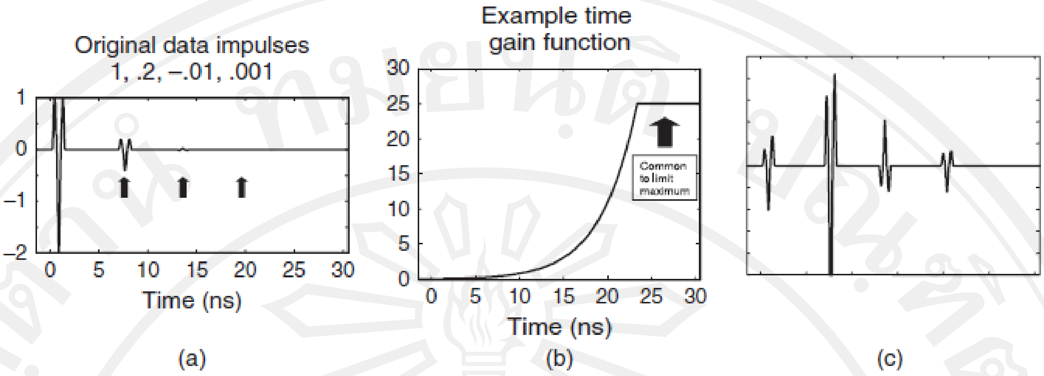

Figure 3.5. Concept of time-varying gain where signal amplification varies with time to compensate for attenuation. (a) a GPR trace with four signals of decreasing amplitude with time, (b) shows a time gain function, (c) shows the result of multiplying (a) by (b). All four events are clearly visible in (c). (From Harry, 2009).

3.6 Deconvolution

Multiple reflections (ringing) are caused by reflections of wave between a buried object and the ground surface, or between subsurface layers. When these reflections are received, they are displayed as repetitive horizontal reflections in profile. Multiples can be confused with real reflections that may be generated from multiple stack layers in the ground. However, multiples can be differentiated because they present the same time interval between multiples. Deconvolution process is used to improve the resolution of sections by compressing the recorded GPR wavelet into a narrow, distinct form (Yilmaz, 2001). In other words, it is used to remove the effect of the source wavelet from the recorded data (Neves et al., 1996) and leave the impulse response of subsurface layers only. It is also used to identify and remove these multiples from the GPR data. After performing deconvolution, reflectors in profile show original pattern like subsurface layers.

3.7 Migration

Steeply dipping reflectors diffract EM wave during its transmission and reflection. Travel time of wave is longer and causes reflections place at incorrect depths or locations. Size and geometry of reflectors also can be changed. Diffraction from the point source results a hyperbola in GPR profile, which distorts real reflections. The migration process can adjust these distortions by collapsing hyperbola to its origin and moves reflectors to correct positions (Figure 3.6). There are several migration algorithms; Kirchhoff, Stolt, phase-shift and finite-difference. In this study Kirchhoff technique (Moran et al., 1998) was employed.

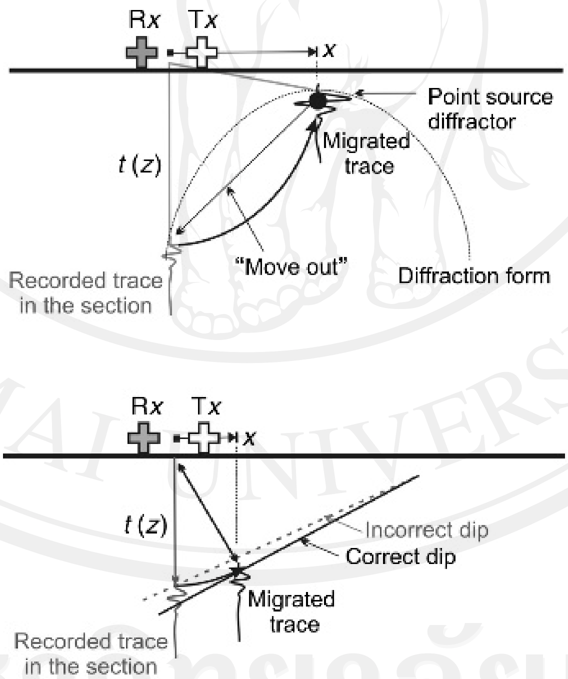

Figure 3.6. Principle of migration attempt to (top) collapse diffraction to the point source and (bottom) move reflected signal back to the right position. (From Harry, 2009).

3.8 GPR Processing of Wat Pan Sao Data Set

3.8.1 Data Preparation

The GPR data from Wat Pan Sao, 35 north-south (inline) and 26 east-west (crossline) profiles were input to the VISTA® software for data processing. Header creating and trace editing were performed before establishing the geometry of each GPR trace. The inline and crossline positions were renumbered to be in hundred times of their real positions so they can be large enough distance to be used and viewed in the VISTA® and the OpendTect software. This is because such programs are originally developed for seismic data which contain different unit scale than the GPR data. For example, a trace spacing of the seismic data is in meter unit but that of the GPR is in centimeter unit and the seismic velocity is in m/s while the GPR velocity is in m/ns. Geometry of the inlines and crosslines of the GPR data from Wat Pan Sao are shown in Figure 3.7.

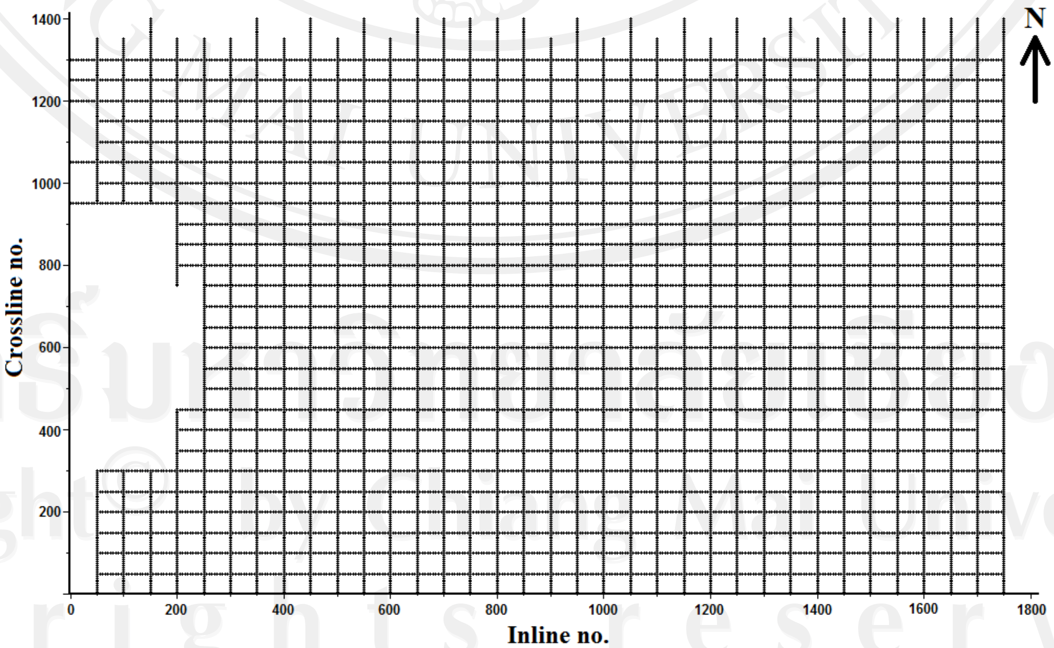

Figure 3.7. Geometry of the GPR data from Wat Pan Sao.

3.8.2 Dewow

The dewow or DC removal was applied to the GPR data from Wat Pan Sao by subtracting all GPR traces with amplitude of 32800, the average amplitude of all GPR traces in the data set at zero time (Figure 3.8). Figure 3.9 presents an example of GPR traces before and after performing dewow.

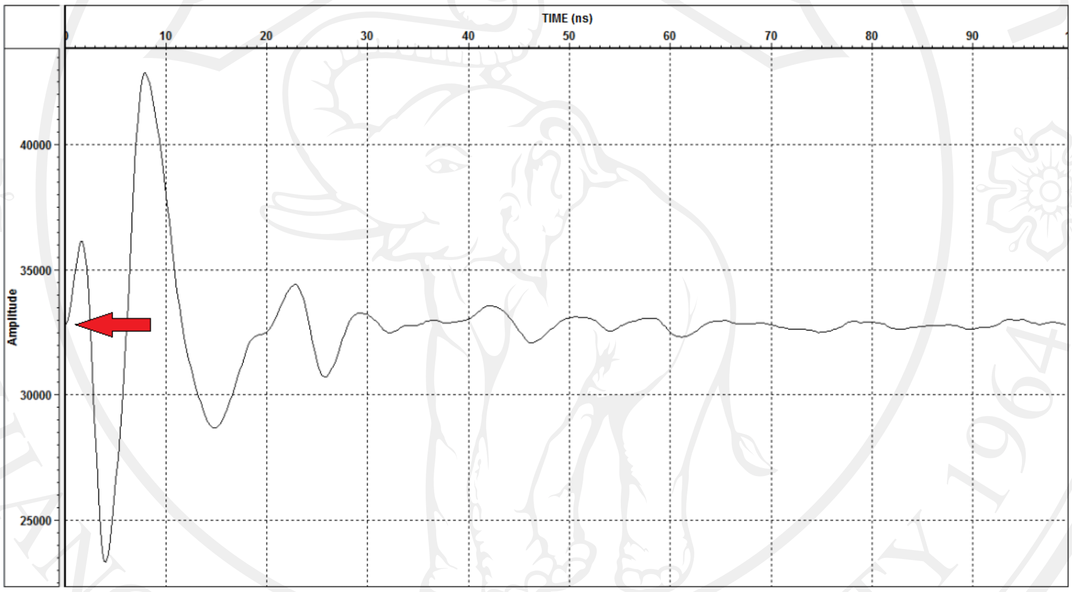

Figure 3.8. Average amplitude trace of all GPR data traces from Wat Pan Sao with the amplitude at zero time of 32800.

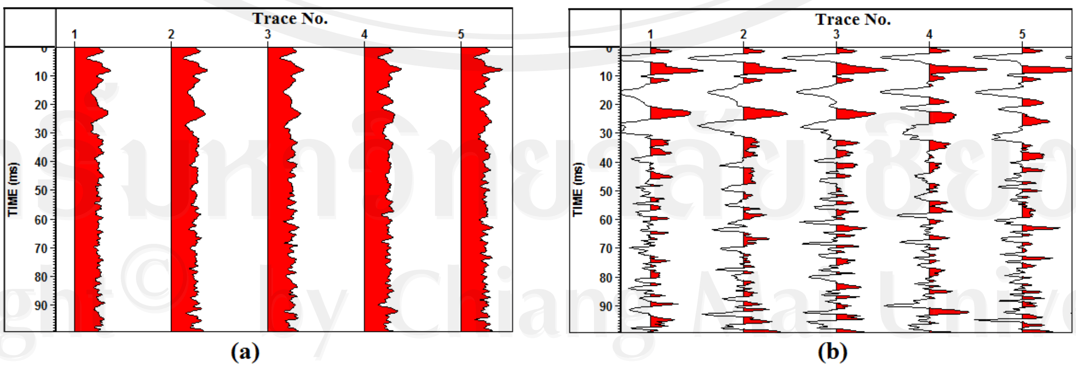

Figure 3.9. Wat Pan Sao GPR traces (a) before and (b) after dewow.

3.8.3 Background Removal

Background removal was applied to all GPR profiles from Wat Pan Sao after performing the dewow to remove continuous flat reflections. Figure 3.10 shows an example GPR profile before and after applying the background removal. With background removal, continuous flat reflections at top of the profile are attenuated and the profile is better imaged.

3.8.4 Frequency Filtering

FK and band-pass frequency filters were used to remove unwanted noise frequency that still includes in the GPR profiles. FK filter zone is presented as shaded area outside the polygon in Figure 3.11. This zone was chosen to be frequency removed at designed wave numbers by examining from the frequency spectrum (F-SUM in Figure 3.11) containing the frequency range of about 50 to 400 MHz. In the f-k domain (Figure 3.11), low value of wave number represents continuous reflector while high value represents segments or discontinuous reflectors. The band-pass filter was performed after the FK filter. A frequency band of 70-120/350-400 MHz was selected after several tests. The GPR data with applying FK and band-pass filters present distinctive continuous reflectors, with high frequency noise attenuated (Figure 3.12).

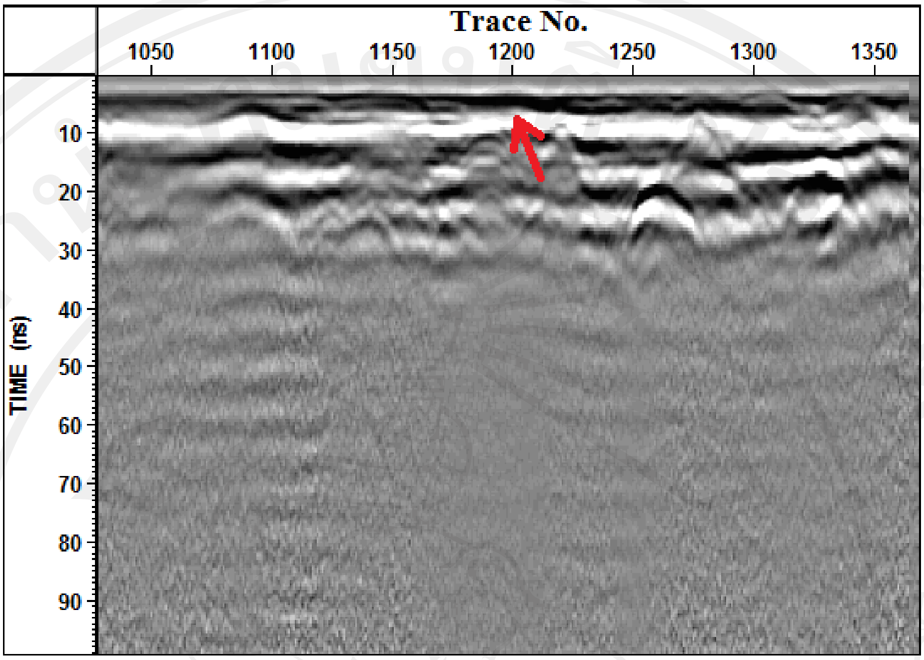

(a)

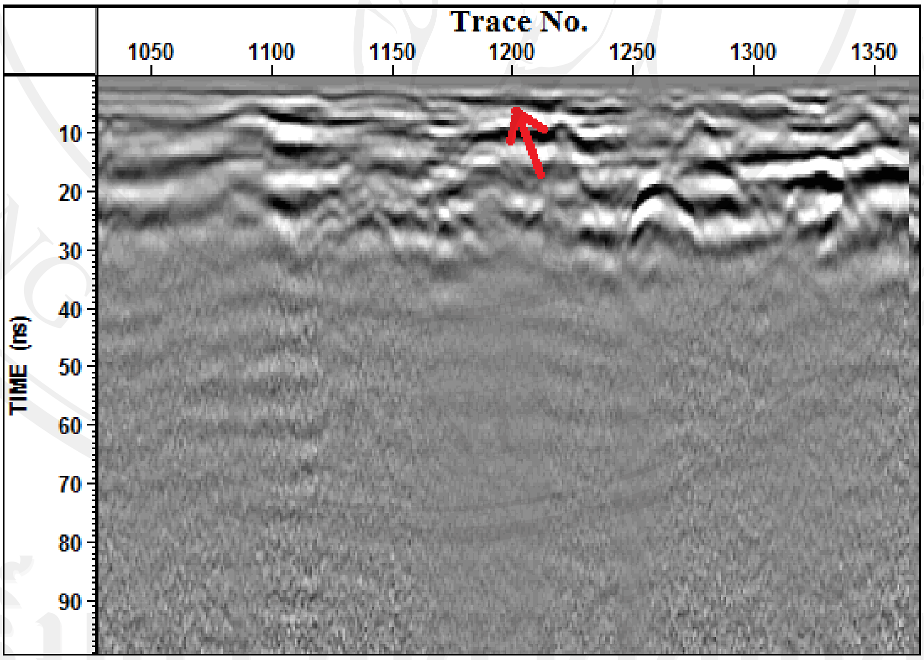

(b)

Figure 3.10. Wat Pan Sao GPR profile at crossline number 200, (a) before and (b) after justified background removal. Red arrow in each profile indicates flat reflection area before and after background removal, respectively.

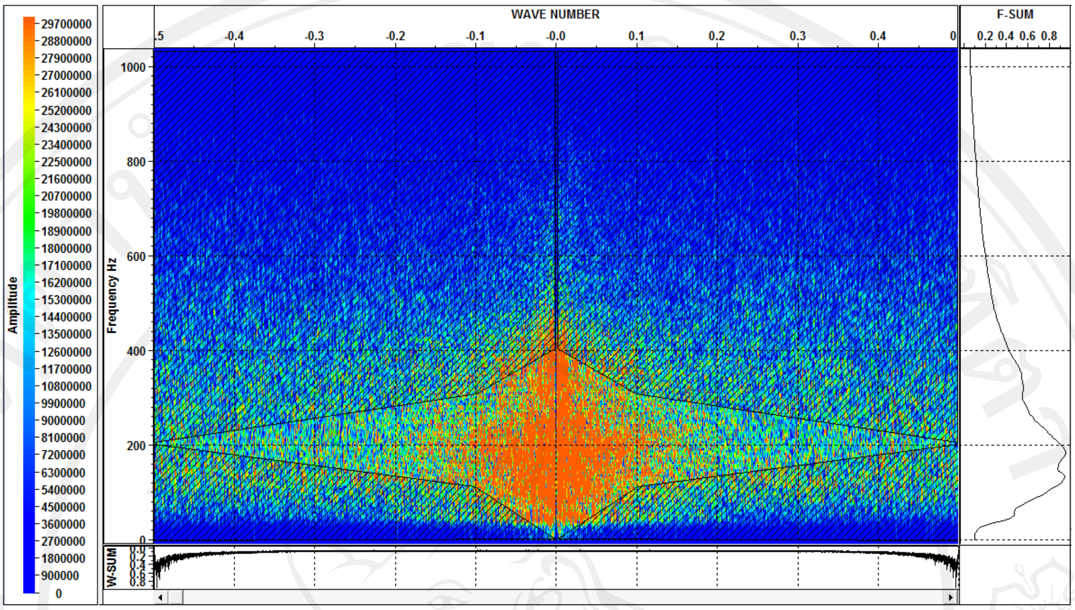

Figure 3.11. Selected f-k filter zone (shade area) of Wat Pan Sao GPR data and frequency spectrum (F-SUM).

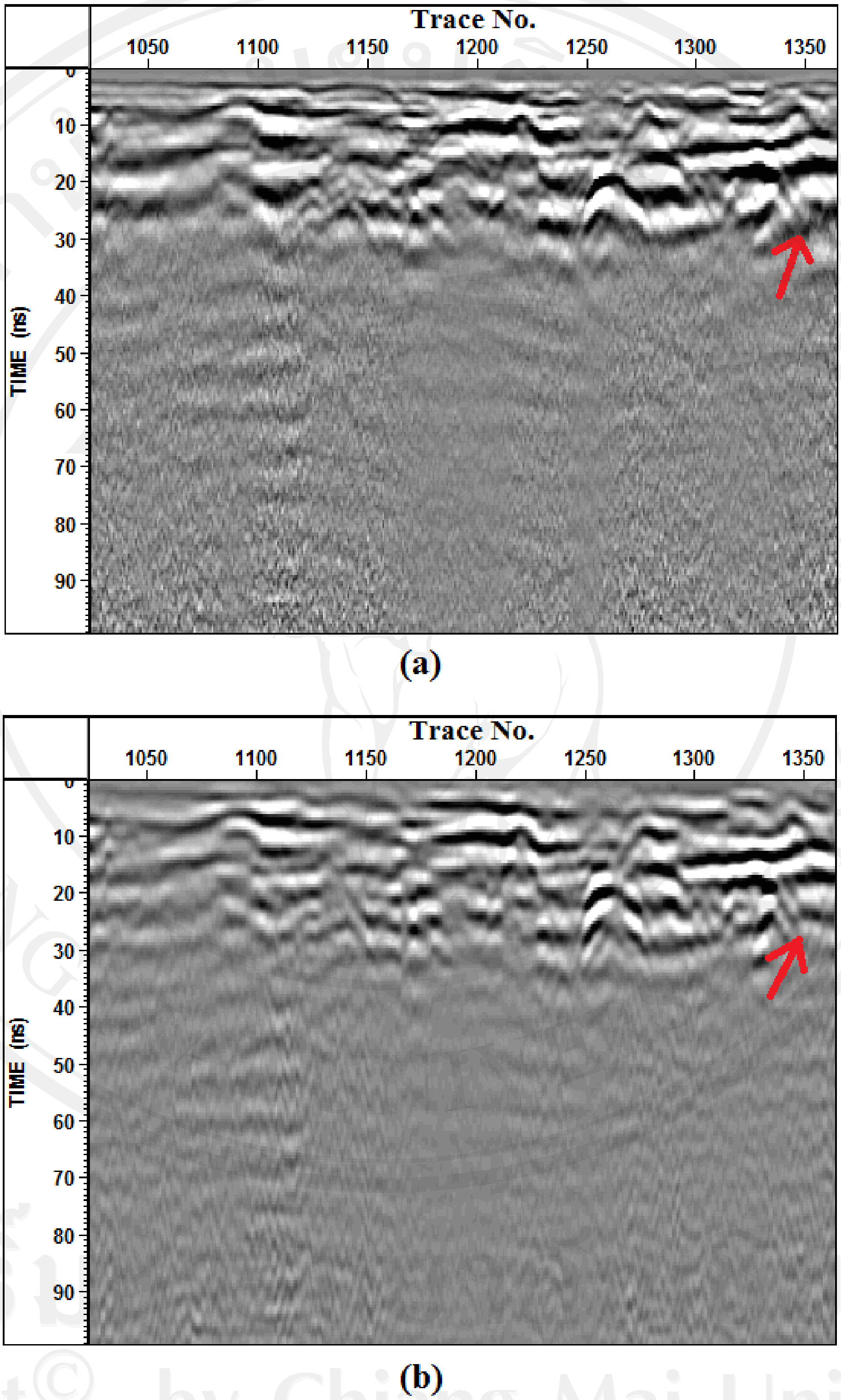

Figure 3.12. Wat Pan Sao GPR profile at crossline number 200 with DC removal and background removal, (a) before and (b) after f-k and band-pass filters. Red arrows highlight distinctive area where noise was attenuated.

3.8.5 Automatic Gain Control

AGC was performed on the GPR data from Wat Pan Sao with sliding window of 80 ns with several tests. Figure 3.13a and 3.13b present a GPR profile before and after AGC. Amplitude and reflectors are clearer presented in the whole profile (Figure 3.13b).

3.8.6 Deconvolution

Autocorrelation was performed to estimate the length of wavelet to be used for the deconvolution processing. The wavelet length, which was estimated from the 2nd zero crossing in Figure 3.14 is 4.55 ns. The window length for the deconvolution which should be 1.5 to 2.0 times of the wavelet length (GEDCO, 2007), for Wat Pan Sao data is 6.825 ns. Predictive deconvolution was applied to the GPR data to improve event reflectors and remove multiple reflections. Figure 3.15 shows an example of a GPR section before and after applying the deconvolution. After applying the predictive deconvolution, multiple reflections are removed, reflectors are sharpened and some reflectors behind multiple reflections are appeared.

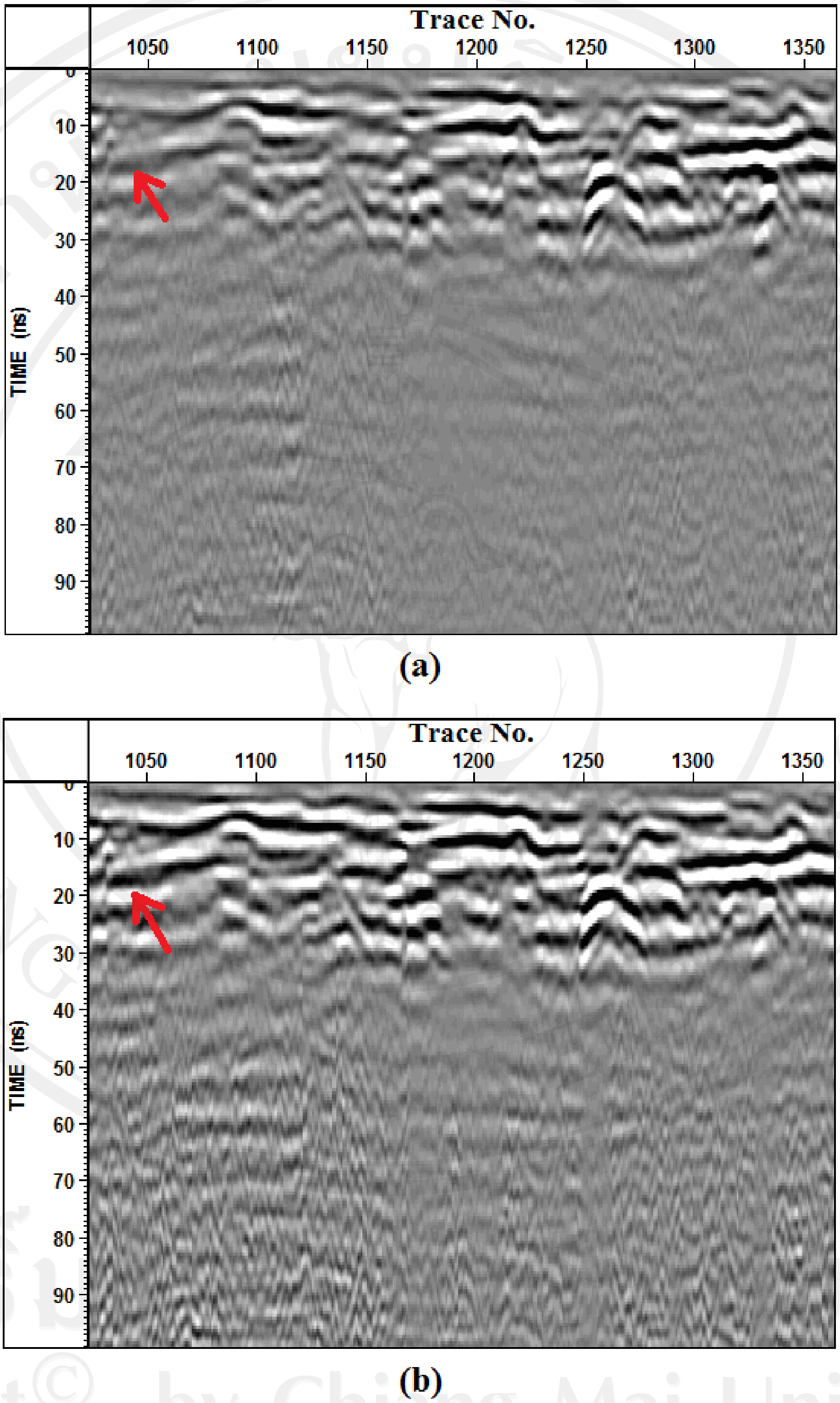

Figure 3.13. Wat Pan Sao GPR profile at crossline number 200, (a) before and (b) after performing automatic gain control. Red arrows highlight distinctive area where noise was attenuated.

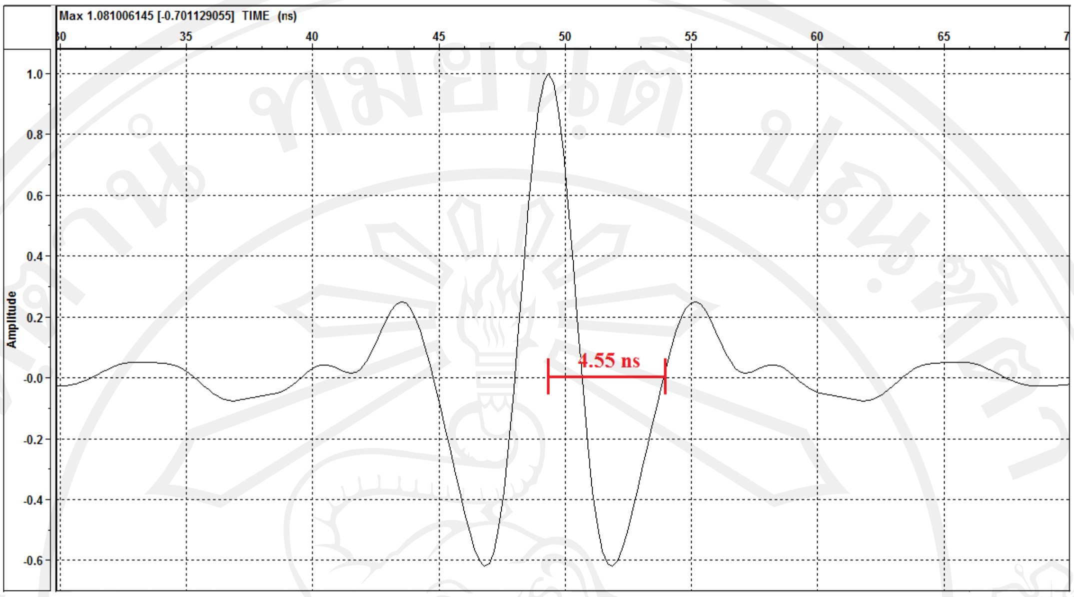

Figure 3.14. Average of all Wat Pan Sao traces autocorrelation with the 2nd zero-crossing of 4.55 ns.

3.8.7 Migration

Kirchhoff post-stack time migration was applied with a constant velocity of 0.09 m/ns. This velocity was estimated from the shapes of diffraction hyperbola. By migrating the data with various constant velocities, the velocity of 0.09 m/ns best collapsed the hyperbola. Figure 3.16 shows an example of GPR profiles before and after applying the migration. It can be seen from Figure 3.16a that a hyperbola presented in the un-migrated profile was removed after the migration. In addition, other small hyperbolas in the section were removed with clearer reflectors presence.

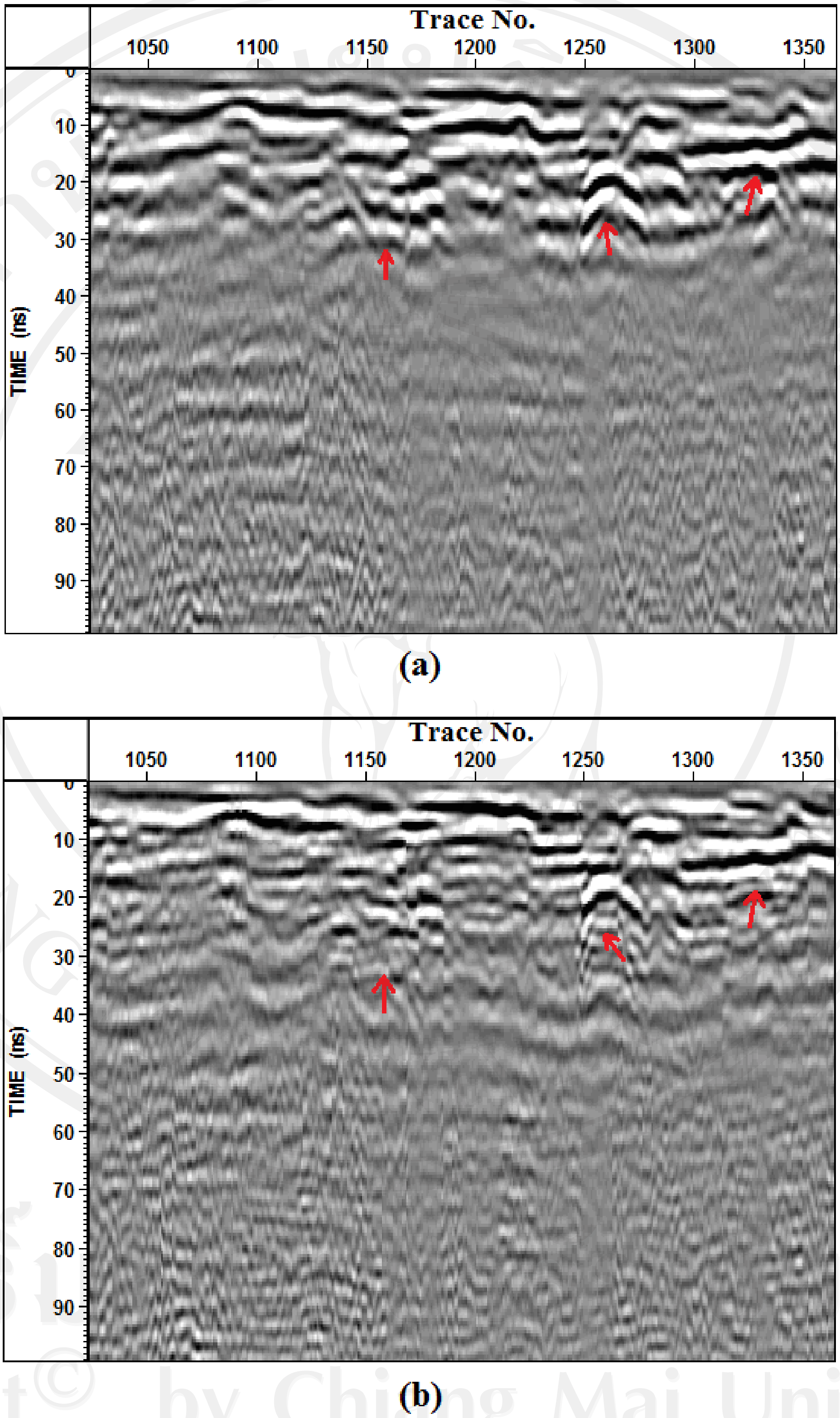

Figure 3.15. Wat Pan Sao GPR profile at crossline number 200, (a) with and (b) without predictive deconvolution. Red arrows highlight areas where multiple reflections are removed, reflectors are sharpened and appeared.

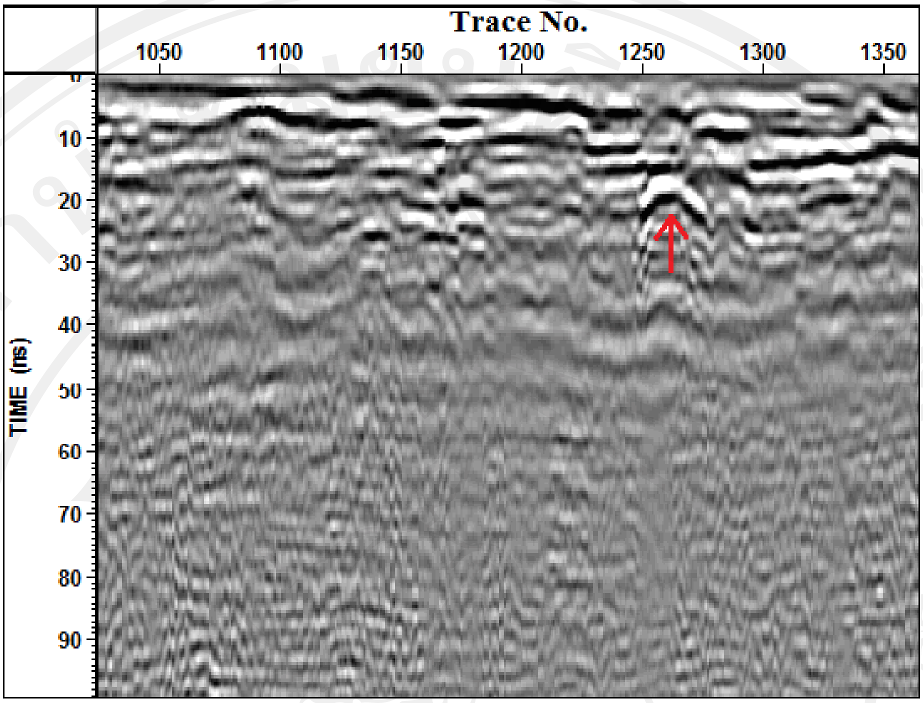

(a)

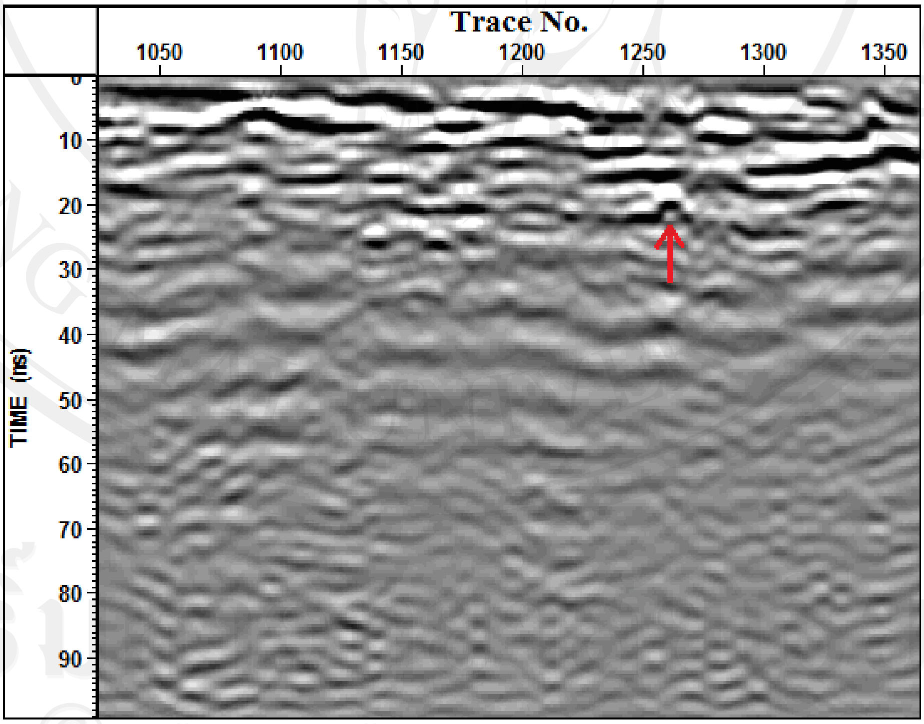

(b)

Figure 3.16. Wat Pan Sao GPR profile at crossline number 200, (a) before and (b) after applying Kirchhoff post-stack time migration. Red arrows indicate an area where hyperbola was collapsed.

3.9 GPR Processing of Wiang Kum Kam Data Set

3.9.1 Data Preparation

The GPR data from Wiang Kum Kam, 19 profiles in the north-south (inline) direction were input to the VISTA® software for data processing. Header creating and trace editing were performed before establishing the geometry of each GPR trace in the same manner as Wat Pan Sao data set. Geometry of Wiang Kum Kam GPR data are presented in Figure 3.17.

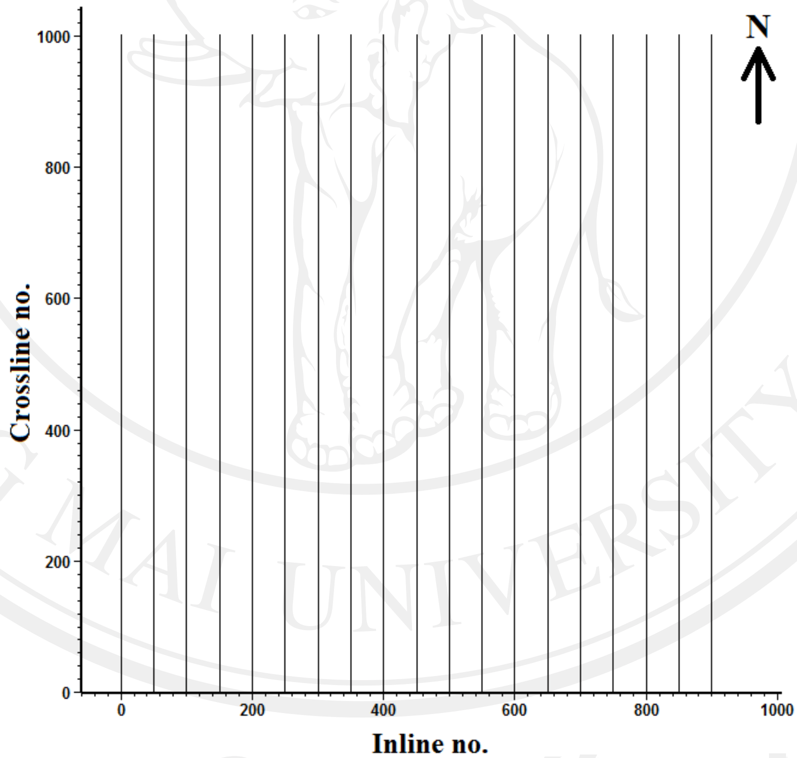

Figure 3.17. Geometry of the GPR data from Wiang Kum Kam.

3.9.2 Dewow

Wiang Kum Kam GPR data traces were subtracted by amplitude of 32771, which is the average amplitude of all traces at zero time (Figure 3.18) for wow removal. Figure 3.19a presents an example of the GPR traces from Wiang Kum Kam before and after applying dewow.

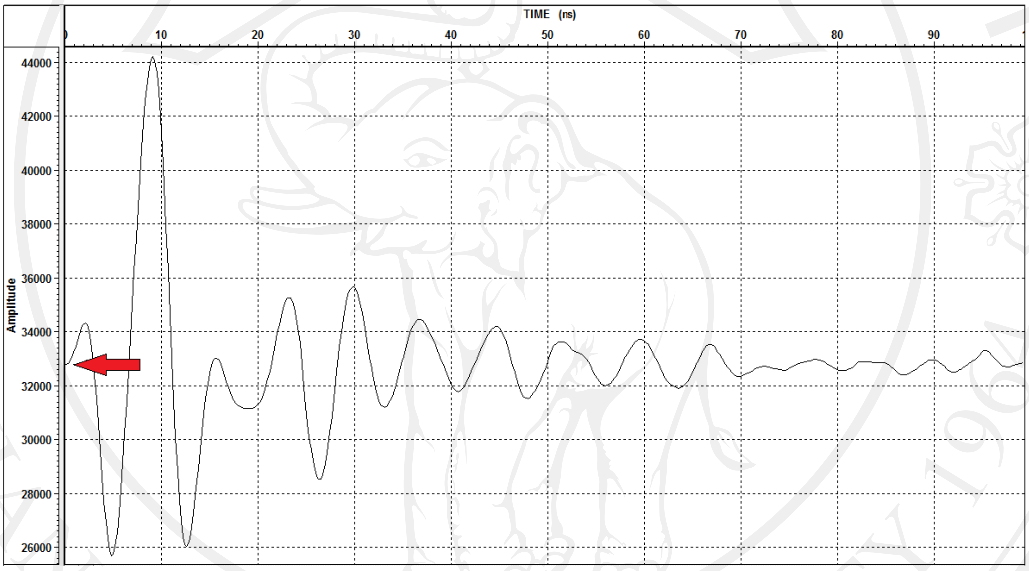

Figure 3.18. Average amplitude trace of Wiang Kum Kam all GPR data traceswith the amplitude at zero time of 32771.

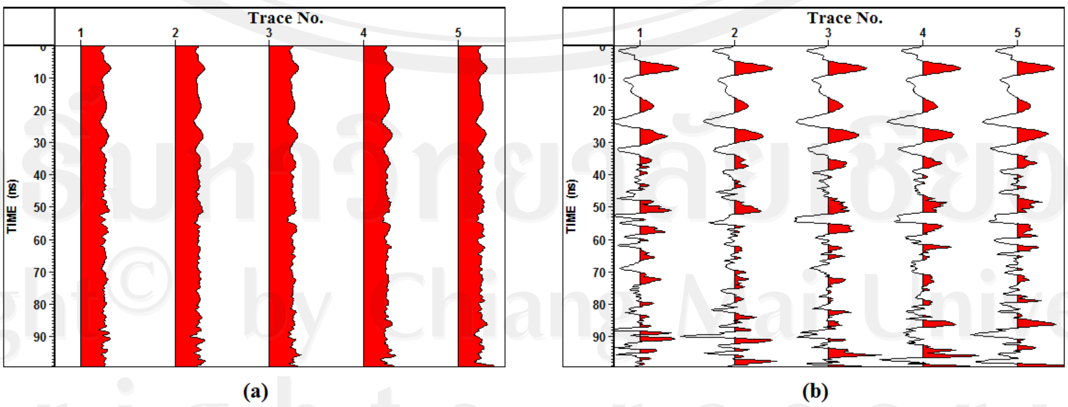

Figure 3.19. Wiang Kum Kam GPR traces (a) before and (b) after DC removal.

3.9.3 Background Removal

Background removal was applied to all GPR profiles from Wiang Kum Kam after performing the dewow to remove continuous flat reflections. Figure 3.20 shows an example of Wiang Kum Kam GPR profile before and after applying the background removal. Figure 3.20a presents GPR data with horizontal event and obscure reflections in the upper part of profile (time 0 – 15 ns). GPR data after background removal in Figure 3.20b shows that horizontal event is reduced and clearer reflectors are presented in the upper part of the profile (time 0 – 15 ns).

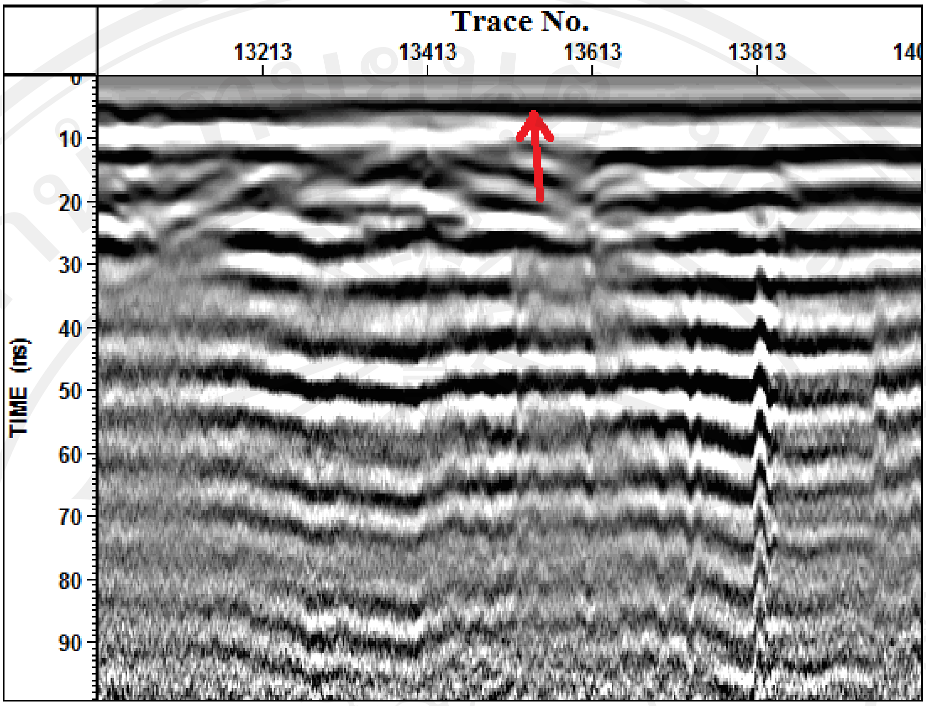

(a)

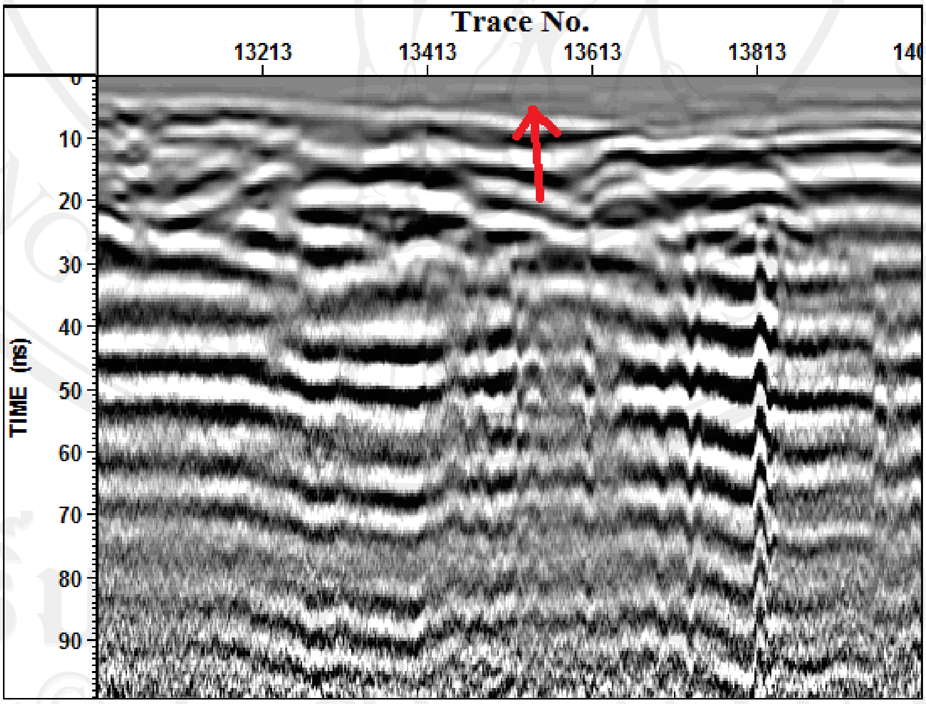

(b)

Figure 3.20. Wiang Kum Kam profile at inline number 651, (a) before and (b) after background removal. Red arrows indicate area where a horizontal reflector is clearly removed.

3.9.4 Frequency Filtering

High and low frequency noises in GPR data from Wiang Kum Kam were removed by FK and band-pass filters. FK filter zone (shaded area outside the polygon in Figure 3.21 was chosen to be frequency removed at designed wave numbers by examining from the frequency spectrum (F-SUM in Figure 3.21) containing the frequency range of about 50 to 350 MHz. The band-pass filter was performed after the FK filter with a frequency band of 80-130/350-400 MHz selected after several testings. Figure 3.22 shows a GPR profile from Wiang Kum Kam before and after applying FK and band-pass filters. With such filters the GPR profile presents distinctive continuous reflectors, with low and high frequency noise attenuated (Figure 3.22b).

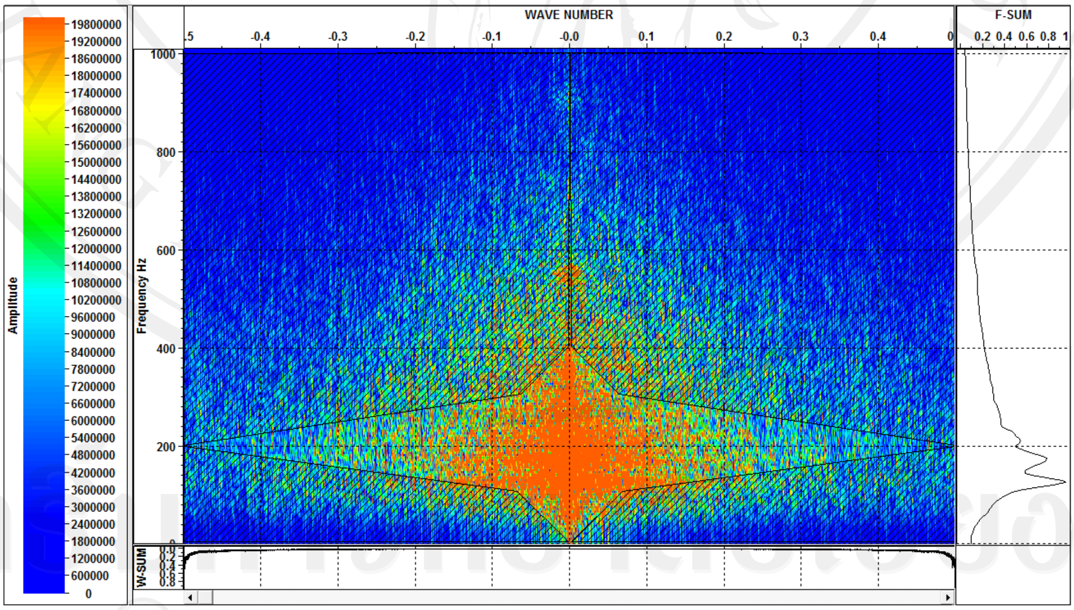

Figure 3.21. Selected f-k filter zone (shaded area) of Wiang Kum Kam GPR data and frequency spectrum (F-SUM).

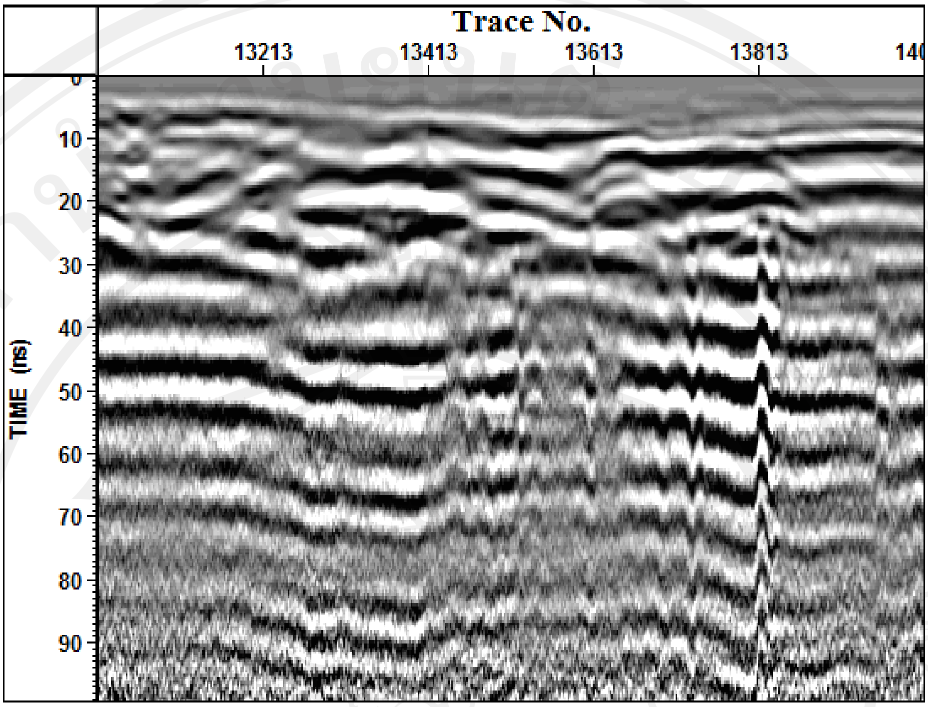

(a)

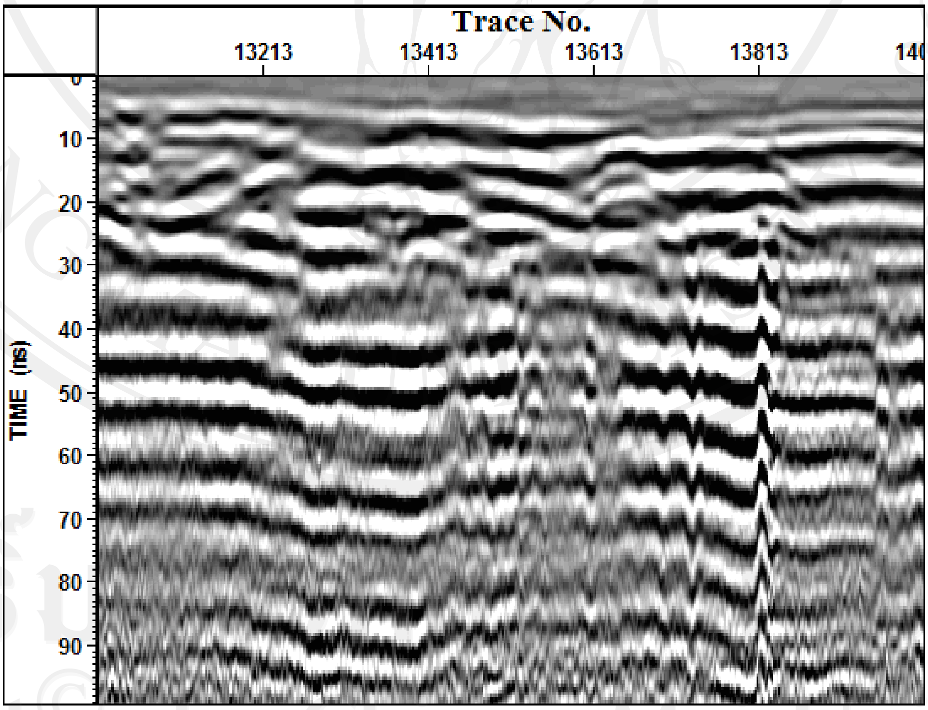

(b)

Figure 3.22. Wiang Kum Kam GPR profile at inline number 651 with DC removal and background removal, (a) before and (b) after f-k and band-pass filters.

3.9.5 Automatic Gain Control

AGC was not applied to the GPR data from Wiang Kum Kam because amplitude of multiples at the deeper part close to reflectors at the shallow part then AGC does not effect to the data.

3.9.6 Deconvolution

The wavelet length of Wiang Kum Kam GPR data from autocorrelation is 4.92 ns (Figure 3.23) yielding the window length for predictive deconvolution of 7.38 ns. An example of Wiang Kum Kam GPR profile before and after performing predictive deconvolution is shown in Figure 3.24. After applying the predictive deconvolution multiples and obscure reflectors are clearly attenuated (Figure 3.24b) however, some small amplitude multiples and small hyperbolas still appear.

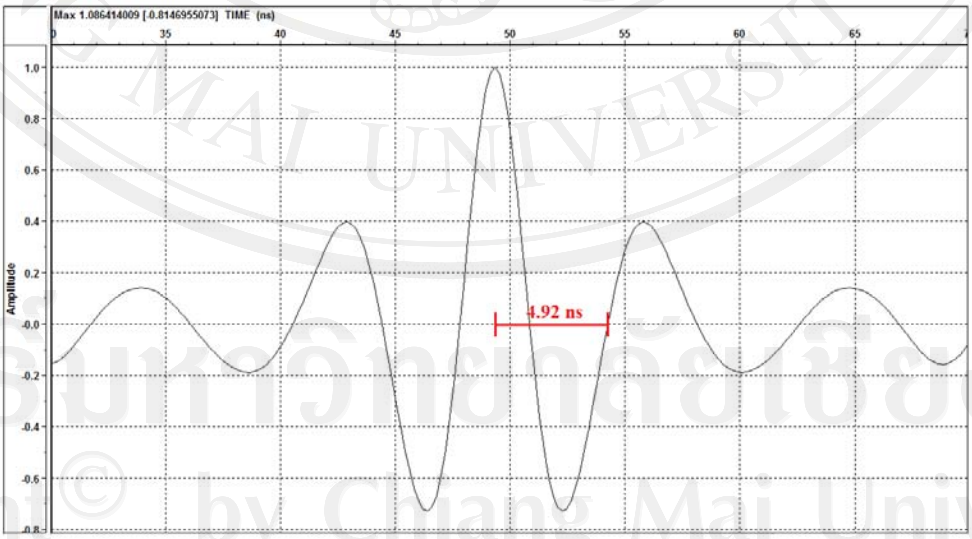

Figure 3.23. Average of all Wiang Kum Kam traces autocorrelation that have 2nd zero-crossing of 4.92 ns.

3.9.7 Migration

A constant velocity of 0.1 m/ns was used in Kirchhoff post-stack time migration for Wiang Kum Kam data set. Such velocity was extracted in the same way as Wat Pan Sao data set. An example of a GPR profile from Wiang Kum Kam with and without the migration is displayed in Figure 3.25. After applying the migration the GPR profile presents much clearer image with distinctive reflectors and small hyperbola attenuations (Figure 3.25b).

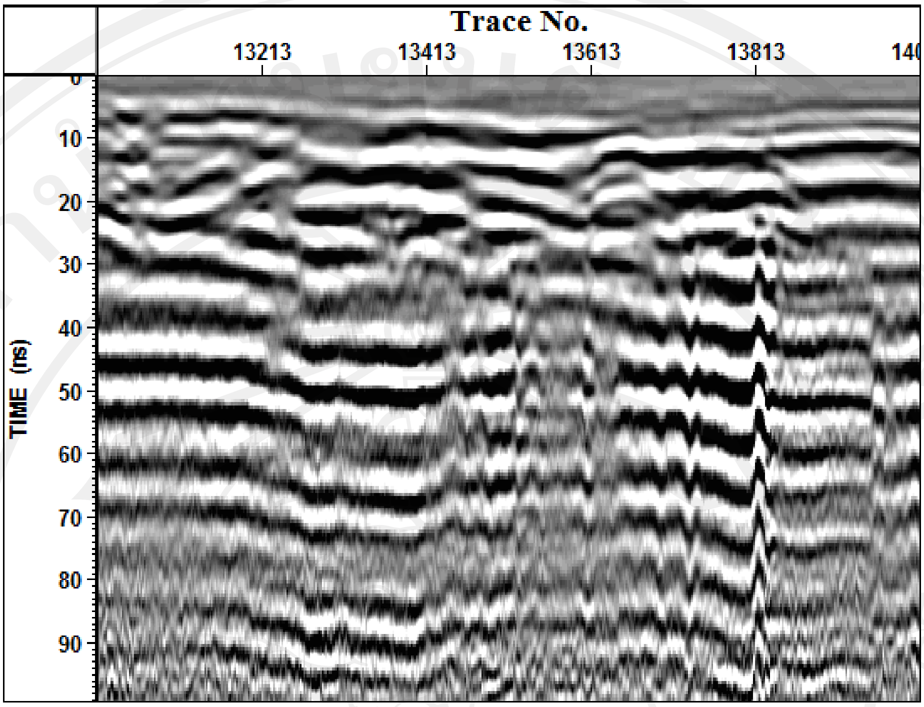

(a)

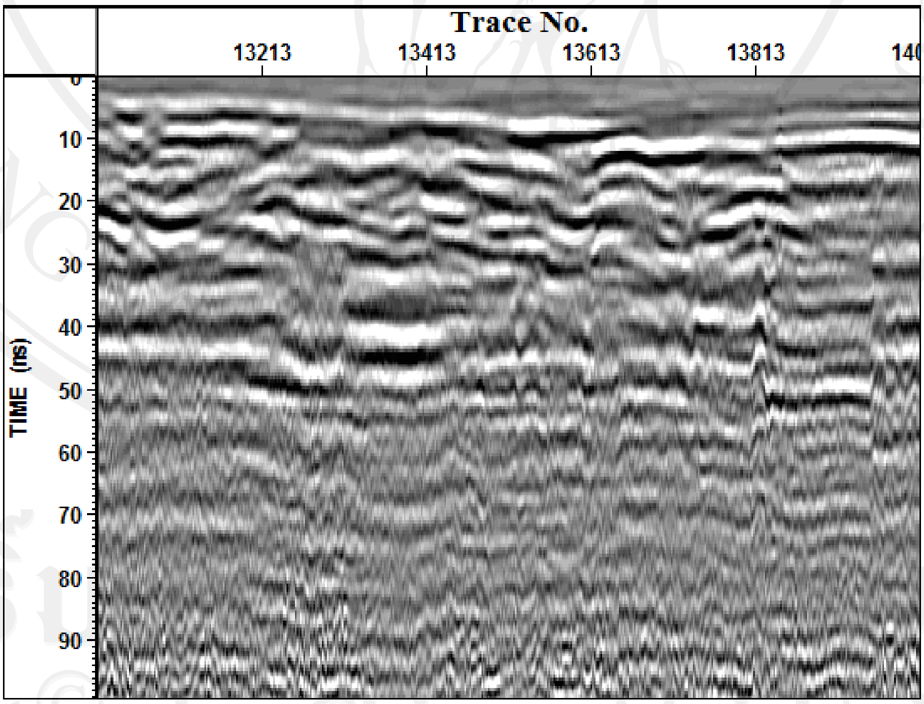

(b)

Figure 3.24. Wiang Kum Kam GPR profile at inline number 651, (a) with and (b) without predictive deconvolution.

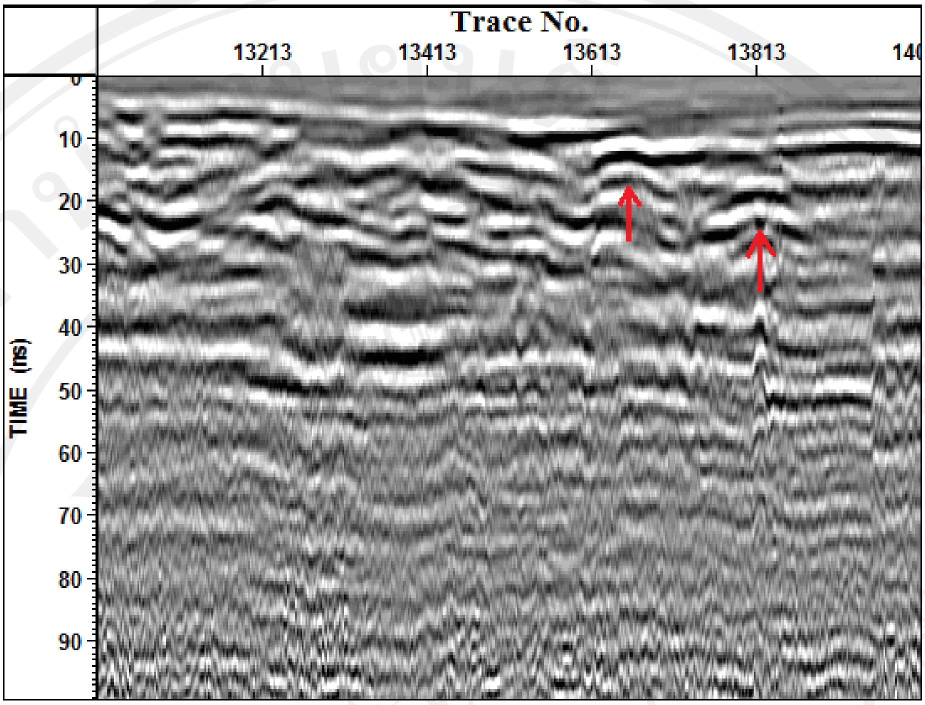

(a)

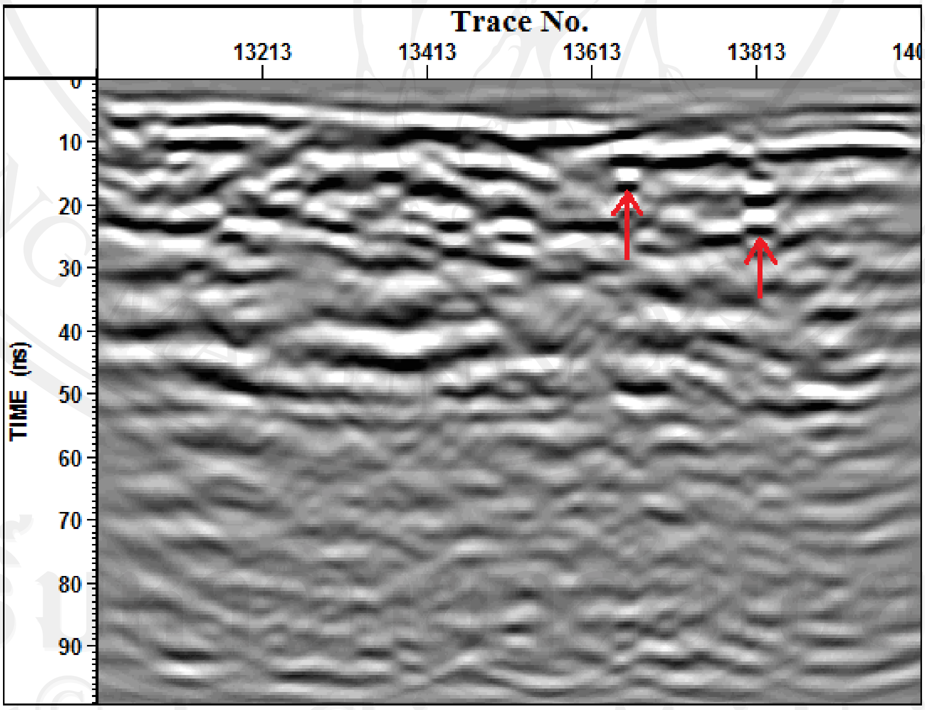

(b)

Figure 3.25. Wiang Kum Kam GPR profile at inline number 651 (a) before and (b) after applying Kirchhoff post-stack time migration. Red arrows highlight areas of hyperbolas attenuated.